

# Hollow Metal Microneedles for Insulin Delivery to Diabetic Rats

Shawn P. Davis, Wijaya Martanto, Mark G. Allen\*, *Senior Member, IEEE*, and Mark R. Prausnitz\*

**Abstract**—The goal of this study was to design, fabricate, and test arrays of hollow microneedles for minimally invasive and continuous delivery of insulin *in vivo*. As a simple, robust fabrication method suitable for inexpensive mass production, we developed a modified-LIGA process to micromachine molds out of polyethylene terephthalate using an ultraviolet laser, coated those molds with nickel by electrodeposition onto a sputter-deposited seed layer, and released the resulting metal microneedle arrays by selectively etching the polymer mold. Mechanical testing showed that these microneedles were sufficiently strong to pierce living skin without breaking. Arrays containing 16 microneedles measuring 500  $\mu\text{m}$  in length with a 75  $\mu\text{m}$  tip diameter were then inserted into the skin of anesthetized, diabetic, hairless rats. Insulin delivery through microneedles caused blood glucose levels to drop steadily to 47% of pretreatment values over a 4-h insulin delivery period and were then approximately constant over a 4-h postdelivery monitoring period. Direct measurement of plasma insulin levels showed a peak value of 0.43 ng/ml. Together, these data suggest that microneedles can be fabricated and used for *in vivo* insulin delivery.

**Index Terms**—Drug delivery systems, laser machining, micromachining.

## I. INTRODUCTION

TREATMENT of type 1 diabetes is severely limited by inadequate methods of insulin delivery [1], [2]. Patients often do not take their insulin at prescribed times due to the pain and inconvenience of hypodermic needle injections. Moreover, hypodermic injection at a small number of discrete time points provides bolus therapy for a disease that would benefit from continuous treatment. For this reason, insulin pump therapy has become increasingly popular because it provides continuous drug delivery. However, insertion and maintenance of the in-dwelling catheter can be problematic for some patients.

An alternate approach is insulin delivery from a transdermal patch, which could provide insulin on a continuous basis using a system likely to be well accepted by patients. However, the extraordinary barrier properties of skin's outer layer, stratum corneum, almost completely block transport of insulin and other

Manuscript received April 23, 2004; revised October 10, 2004. This work was supported in part by the American Diabetes Association and National Institutes of Health. *Asterisks indicate corresponding authors.*

S. P. Davis was with the School of Chemical & Biomolecular Engineering, Georgia Institute of Technology, Atlanta, GA 30332 USA and is currently with Milliken Research Corporation, Spartanburg, SC 29304 USA (e-mail: shawn.davis@milliken.com).

W. S. Martanto is with the School of Chemical & Biomolecular Engineering, Georgia Institute of Technology, Atlanta, GA 30332 USA.

\*M. G. Allen is with the School of Electrical and Computer Engineering, Georgia Institute of Technology, Atlanta, GA 30332 USA (e-mail: mark.allen@ece.gatech.edu).

\*M. R. Prausnitz is with the School of Chemical & Biomolecular Engineering, Georgia Institute of Technology, Atlanta, GA 30332 USA (e-mail: mark.prausnitz@chbe.gatech.edu).

Digital Object Identifier 10.1109/TBME.2005.845240

large therapeutic molecules. Chemical, electrical, ultrasonic and other methods to increase transdermal insulin delivery have had some success [3], [4].

As a hybrid between hypodermic needles and transdermal patches, we have proposed that arrays of microscopic needles can be used to pierce into the upper layers of skin and thereby provide minimally invasive conduits for insulin transport for uptake by the dermal capillaries for systemic administration. In a diffusion-based system, evaluated in this study, basal levels of insulin could be provided by microneedles, which in some cases may need to be supplemented with meal-time bolus delivery. Although beyond the scope of this study, insulin solutions could also be pumped through hollow microneedles in a manner similar to current insulin pumps, but with the use of a minimally invasive microneedle array rather than an in-dwelling catheter.

Using the tools of the microelectronics industry, we and others have fabricated solid microneedles out of metal and silicon [5]–[7] for *in vitro* delivery of a range of compounds and *in vivo* delivery of oligonucleotides, as well as DNA- and protein-antigen vaccines [8]–[12]. These solid microneedles act by piercing holes in the skin through which drug can be transported either from a patch-like reservoir on the skin surface or for release from a coating on the microneedle surface. Additional work showed that microneedles are perceived as painless by human subjects [13].

To expand upon the drug delivery capabilities of solid microneedles, hollow microneedles have also been created [14]–[17]. In this study, we build off our previous work [17]–[19] to provide detailed methods for a novel fabrication process that creates arrays of hollow metal microneedles for transdermal delivery of insulin using a method suitable for rapid scale-up for low-cost mass production. *In vivo* studies demonstrating insertion of microneedles into skin and delivery of insulin to modulate the blood glucose level of diabetic rats are also reported.

## II. METHODS

### A. Microneedle Fabrication

Hollow metal microneedles were created from polymer molds as shown schematically in Fig. 1. To make the molds, an ultraviolet laser (Resonetics Micromaster, Nashua, NH) was used to drill holes through sheets of polyethylene terephthalate (Mylar, Dupont, Wilmington, DE) as shown in Fig. 1(a). Tapered holes were made to produce conical needles; straight-walled holes were also made to produce cylindrical tubes. Mylar was chosen as the mold material for its ease of removal after microneedle formation and its relatively

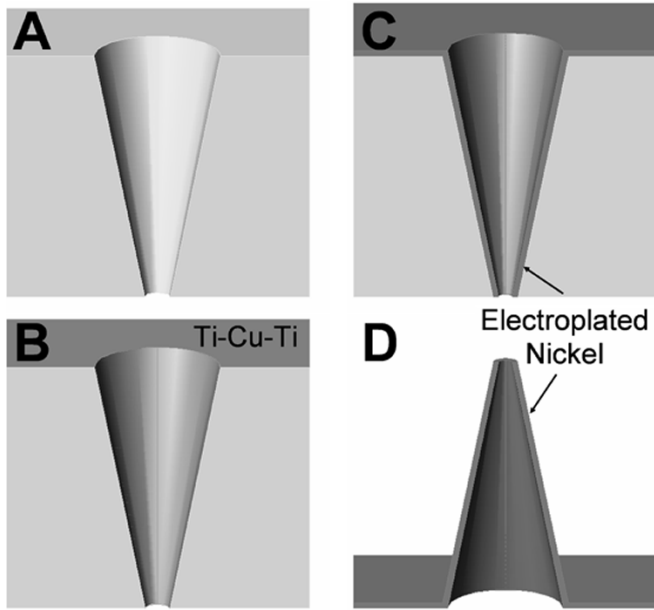


Fig. 1. Schematic sequence of the microneedle fabrication process using a polymer mold: (a) tapered holes are laser drilled through a polymer substrate, (b) a conductive seed layer is deposited on the top and sidewalls of the mold, (c) metal is electroplated onto the seed layer and (d) the mold is selectively wet etched to release the metal microneedles.

inexpensive cost. The laser was operated at 200 Hz with a 248-nm wavelength and a typical energy density of  $2.0 \text{ J/cm}^2$ .

The relatively flat energy profile of the excimer beam allows physical masking to produce a circular pattern for drilling. To give the drilled holes a tapered geometry, the drilling program was set to trepan, or trace, a circular path with a diameter less than the diameter of the circular laser beam, as shown in Fig. 2. In this way, a circular region of strong laser fluence was generated in the center and an annular region of weaker fluence was generated around it, which produced a tapered hole. To achieve a needle mold with a desired base diameter ( $d_{\text{base}}$ ) and tip diameter ( $d_{\text{tip}}$ ), the following expressions were used to determine the required laser beam diameter ( $d_{\text{beam}}$ ) and trepan diameter ( $d_{\text{trepan}}$ ).

$$d_{\text{beam}} = \frac{d_{\text{tip}} + d_{\text{base}}}{2} \quad (1)$$

$$d_{\text{trepan}} = d_{\text{beam}} - d_{\text{tip}}. \quad (2)$$

These parameters, combined with the thickness of the Mylar substrate, which governed the needle mold length, determined the final microneedle geometry. The geometry used for *in vivo* experiments in this study had a  $300\text{-}\mu\text{m}$  base diameter and a  $75\text{-}\mu\text{m}$  tip diameter through a  $500\text{-}\mu\text{m}$  sheet. This corresponded to a  $187.5\text{-}\mu\text{m}$  beam diameter and a  $112.5\text{-}\mu\text{m}$  trepan diameter.

After laser-drilling the mold, a conductive seed layer was deposited on the top and sidewalls of the polymer mold as shown in Fig. 1(b). A typical seed layer was composed of titanium-copper-titanium at thicknesses of 35 nm, 650 nm and 35 nm, respectively, which were deposited by direct-current sputtering (CVC 601, Rochester, NY). The conductive seed layer allowed electroplating of the insulating polymer mold.

Nickel was electroplated onto the mold to create a microneedle as shown in Fig. 1(c). The electroplating was

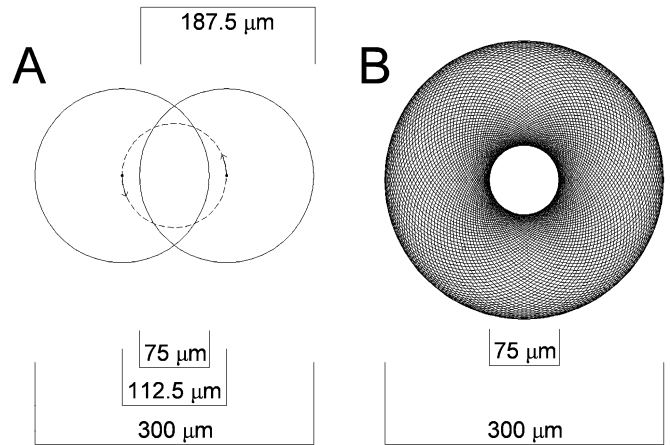


Fig. 2. Illustration of laser trepanning technique. A  $187.5\text{-}\mu\text{m}$  diameter laser beam trepanned in a circular motion with a diameter of only  $112.5\text{-}\mu\text{m}$ . This resulted in a  $300\text{-}\mu\text{m}$  entrance hole, defined by the outer edge of the trepan pattern, and a  $75\text{-}\mu\text{m}$  exit hole in the center, defined by the overlap region irradiated by the laser at all positions along the trepan path. (a) The beam pattern (solid line) shown at two points along the circular trepanned path (dashed line). (b) The overlap of multiple beam pulses along the trepan path define the ultimate drilled pattern. The difference between the beam and trepan diameters results in an overlap region  $75\text{-}\mu\text{m}$  in diameter at the center of the pattern. The overlap region defines the exit hole of the tapered hole (i.e., complete drilling through the substrate), while the entrance hole is defined by the outside edges of the beam diameter during the trepanning.

conducted using a Watts formulation bath (Technic, Cranston, RI) at  $54\text{ }^\circ\text{C}$  [20]. The voltage was adjusted to maintain a constant current density of  $10 \text{ mA/cm}^2$ . Plating proceeded for 5 min under these conditions to form the initial “strike” layer on the mold. The mold was then removed from the bath and rinsed in DI water. A sheet of powder coating tape (Shercon, Santa Fe Springs, CA) was then placed across the bottom of the mold to prevent over-plating at the microneedle tip due to current crowding. The duration of plating determined the thickness of the microneedle walls and the array’s base. A typical plating time was 60 min to generate a  $10\text{-}\mu\text{m}$  thick wall layer of nickel.

Metal microneedle arrays were released from polymer molds in the final step of production, Fig. 1(d). Mylar molds were removed in a concentrated caustic solution (1 N NaOH, boiling) after approximately 20 min for a  $500\text{-}\mu\text{m}$  thick mold.

### B. Microneedle Mechanics

Using methods described previously [18], the force required to insert a microneedle into the skin and the force required to fracture a microneedle were measured and compared. Fracture forces were determined by pressing single microneedles against a metal block and measuring the force applied upon needle failure using an axial load test station (ScopeTest1, EnduraTEC, Minnetonka, MN).

Microneedle insertion forces were determined by pressing single microneedles against the skin on the hand of human subjects and measuring the force applied upon penetration using a displacement-force workstation (Model 921A, Tricor Systems, Elgin, IL). The point of insertion was identified by a sharp drop in skin resistance as the needle pierced across the skin’s outer, high-resistance layer of stratum corneum. Microneedle insertion tests were performed on three Caucasian male subjects who

ranged in age from 20 to 26 years old and gave informed consent. The protocol was approved by the Georgia Institute of Technology Institutional Review Board.

### C. *In Vivo Insulin Delivery*

To assess the ability of microneedles to deliver insulin and modulate blood sugar levels in a diabetic animal, diabetes was induced in male Sprague Dawley hairless rats (250–350 g, Charles River Laboratories, Wilmington, MA) by intravenous injection of 100 mg/kg streptozotocin (Pfanstiehl Laboratories, Waukegan, IL) into the tail vein [21]. The next day, blood glucose levels were measured (Accu-Chek Compact; Roche Diagnostics, Indianapolis, IN) to confirm hyperglycemia (300–550 mg/dl) due to pancreatic islet destruction. Anesthesia was induced by intraperitoneal injection of 1300 mg/kg urethane (Sigma, St. Louis, MO). All procedures were approved by the Georgia Tech Institutional Animal Care and Use Committee and in accordance with the NIH “Principles of Laboratory Animal Care.”

Transdermal insulin delivery experiments were carried out by inserting a microneedle array into the skin of an anesthetized, diabetic, hairless rat with a pneumatic plunger at 30 psi ( $\sim 10$  m/s) (Bionic Technologies, Salt Lake City, UT). A 6-mm diameter, flanged, glass chamber was then adhered (Loctite, Rocky Hill, CT) to the base of the array and the surrounding skin to create a drug reservoir, which was filled with approximately 2 ml of 100 U/ml insulin (Humulin R, Eli Lilly, Indianapolis, IN). In this setup, drug solution was not in direct contact with skin; insulin could transport into the skin only through the hollow bores of the microneedles. As a negative control, the insulin reservoir was placed directly onto intact skin without microneedles and insulin solution was added. As positive controls, 50 and 500 mU of insulin were injected subcutaneously using a 29-gauge hypodermic needle and syringe (Becton Dickinson, Franklin Lakes, NJ).

To measure changes in blood glucose level, a single 10- $\mu$ l blood sample was collected by tail vein laceration every 30 min for 8 h from each rat and assayed using a glucose test strip (Accu-Chek Compact). Insulin was kept in the reservoir during a 4-h delivery period, after which the reservoir was emptied and rats were monitored for an additional 4 h, after which they were sacrificed.

In a separate set of experiments, plasma insulin concentration was measured by collecting two 0.5-ml blood samples: an orbital collection 30 min after starting insulin delivery and an intracardiac collection at 4 h at the time of animal sacrifice. Blood samples were immediately centrifuged at  $2040 \times g$  (Eppendorf Centrifuge 5415C, Westbury, NY) for 5 min and the plasma was stored at  $-70$  °C. The concentration of human insulin (i.e., Humulin R) was determined by radioimmunoassay (Linco Research, St. Charles, MO).

## III. RESULTS AND DISCUSSION

### A. *Microneedle Design*

To produce microneedles useful for insulin delivery, we identified three design constraints that were addressed in this study:

- 1) the needle geometry and material must permit insertion into skin without breaking the needles; 2) the fabrication method should be capable of rapid scale up for inexpensive mass production; 3) the device must be able to transport biologically effective amounts of insulin into the body. Additional issues, such as biocompatibility and lack of pain during use, were also taken into account, but were not addressed in detail in this study.

Our first consideration concerned which microneedle geometry should be used to provide easy insertion. We previously showed that the force of insertion into skin is independent of the base diameter and taper of the needle, but depends linearly on the interfacial area of the needle tip [26]. We, therefore, wanted a tip with a small diameter. However, tip diameter needed to be sufficiently large to permit transport of drug and to be fabricated using simple, robust methods. Based on these constraints, we selected an outer tip diameter of 75  $\mu$ m.

Microneedle insertion also depends on needle length and spacing, where short needles and closely spaced needles cannot overcome the elastic deformation of skin and just dimple the skin without piercing. This limitation can be partially overcome by insertion at high velocity [22]. We, therefore, wanted widely spaced, long needles that are inserted quickly. However, longer needles cause pain and widely spaced needles require a larger device. Based on these constraints, we selected a needle length of 500  $\mu$ m, needle-to-needle spacing of 600  $\mu$ m, and insertion using a commercial device operating at approximately 10 m/s.

We also previously found that the force of microneedle fracture depends strongly on needle wall thickness and needle material [18]. We, therefore, wanted thick walls and a strong material. However, wall thickness had to be thin enough to keep an open lumen at the needle tip and the material needed to be biocompatible and conducive to fabrication. Based on these constraints, we selected a wall thickness of 10  $\mu$ m and the material as nickel, to serve as a representative metal. Although nickel can cause skin irritation for individuals with nickel allergy, it does not pose more significant safety concerns [23].

Microneedle geometry was further constrained by the fabrication process. As discussed below, the polymer molds needed to be sputter coated with a conductive seed layer for subsequent electroplating. Because the sputtering system has difficulty coating the sidewalls of long, narrow holes, the needle mold was required to be tapered in order to expose the complete needle mold surface. Based on this constraint, we selected an outer diameter of 300  $\mu$ m at the needle base, which provided an average taper angle of  $12.7^\circ$  relative to the central needle axis.

### B. *Microneedle Fabrication*

Microneedles with the geometry described above were fabricated using a process involving laser drilling a polymer mold, coating the mold with a conductive seed layer, electroplating the mold with metal, and finally releasing the resulting metal microneedle array by selectively wet etching the mold (Fig. 1). This process was chosen not only for its ability to form needles of the desired geometry but also for its scalability and low expected processing costs. Mylar is a far less expensive mold material in comparison to the common choice of silicon. Laser machining with an excimer beam allows semi-batch processing

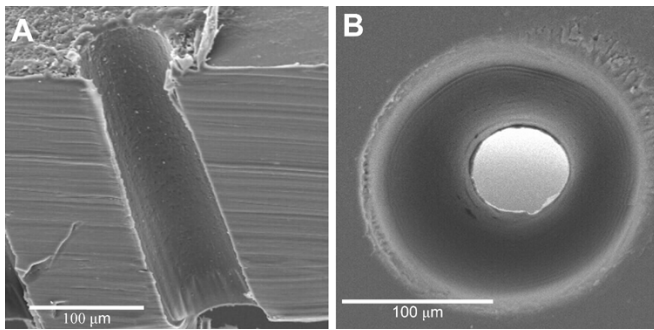


Fig. 3. Mylar molds used to make microneedles. Laser drilling was used to generate (a) a straight-walled hole, viewed in cross-section after sectioning with a blade, or (b) a conically tapered hole formed using a laser trepanning technique, viewed from above. Images from scanning electron microscopy.

rather than the serial processing often associated with laser machining. The relatively flat energy profile of the laser beam permits simultaneous machining of multiple spots within a single beam. In a commercial process, the likely use of a larger cavity, or even multiple cavities, would increase the size and number of beams, thereby increasing the number of holes per pass. Scale up to a roll-to-roll process would increase parallel-processing efficiency still further. Using wet etching to remove the mold from completed needles is also much faster and involves less expensive processing and capital costs than dry etching materials using conventional MEMS techniques. Finally, this process is relatively insensitive to contamination and, therefore, does not require a cleanroom environment, and the associated costs. Assuming large-scale production (e.g., many millions of units), we estimate needle arrays could be manufactured for well under one dollar each, and possibly for less than ten cents (calculation not shown).

Fig. 3 displays images of holes drilled into a Mylar sheet to serve as the mold for a microneedle. Fig. 3(a) shows a representative straight-channel hole with smooth sidewalls and very little re-deposited slag. The slag present on the topside of the mold can easily be removed with methanol and manual wiping. Due to limitations of sputter deposition, molds of this geometry could only be used for short needles (i.e., length-to-width aspect ratios less than 1.6).

To provide molds for longer needles, Fig. 3(b) shows a representative tapered hole, also with a smooth, clean profile, that can be conformally sputter coated with a conductive seed layer. This tapered geometry was achieved by trepanning the laser beam in a circular path whose diameter was less than the diameter of the circular beam. The difference between the beam diameter and the trepanned diameter created a high-fluence region of beam overlap in the center of the pattern and progressively lower energy toward its rim, thereby drilling a tapered hole.

Electrodeposition onto molds like those shown in Fig. 3 yielded metal microneedles. For example, Fig. 4(a) shows a short (180  $\mu\text{m}$ ), nontapered microneedle with an aspect ratio of 1.4 and Fig. 4(b) shows a longer (500  $\mu\text{m}$ ), tapered microneedle with an aspect ratio of 5.0 (i.e., the ratio of needle length to tip diameter). Using this approach, needles having a variety of geometries have been fabricated with diameters of 50–400  $\mu\text{m}$ , lengths of 50–1000  $\mu\text{m}$ , taper angles of 3–45°, aspect ratios up

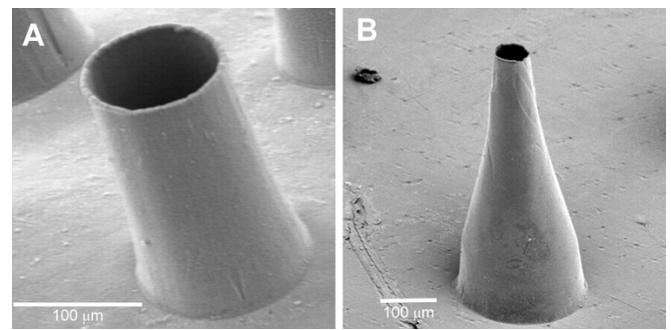


Fig. 4. Hollow, metal microneedles created from polymer molds. (a) A microneedle created from a straight-walled mold. This microneedle has a diameter of 125  $\mu\text{m}$  and is 180  $\mu\text{m}$  tall. (b) A microneedle created from a tapered mold formed using laser trepanning. This microneedle has a base diameter of 250  $\mu\text{m}$ , a tip diameter of 50  $\mu\text{m}$ , and is 500  $\mu\text{m}$  tall. Images from scanning electron microscopy.

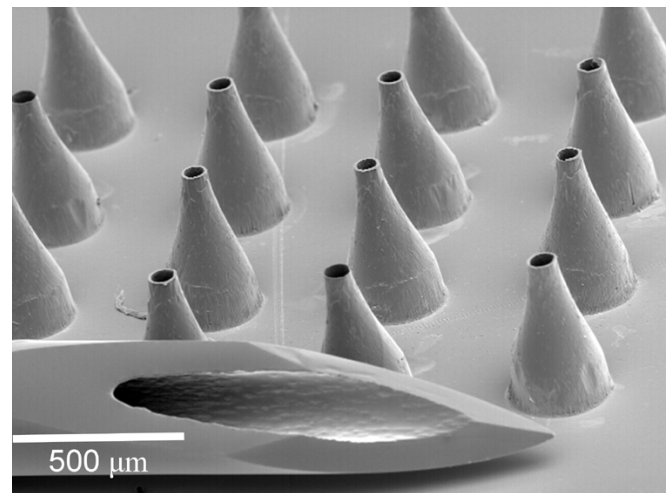


Fig. 5. An array of hollow, metal microneedles shown next to a 27-gauge hypodermic needle. The microneedles taper from a 300- $\mu\text{m}$  base to a tip diameter of 75  $\mu\text{m}$  over a 500- $\mu\text{m}$  length and are arranged in a 4  $\times$  4 array (i.e., 16 needles). Arrays of this geometry were used for insulin delivery experiments. Image from scanning electron microscopy.

to 19, and wall thicknesses of 2–20  $\mu\text{m}$  (data not shown). Most needles have been made out of nickel, but we have also made them out of nickel-iron and gold. In general, we have observed that needle geometries are identical to mold geometries and that needle geometries are consistent within multi-needle arrays and among needle arrays fabricated on different days. To date, we have fabricated close to one thousand microneedle devices using this technique and find it to be very reliable.

For many applications, multi-needle microneedle arrays are especially interesting, because they can deliver more drug and provide redundancy not offered by single needles. Fig. 5 shows an array of microneedles each with a height of 500  $\mu\text{m}$ , base diameter of 300  $\mu\text{m}$ , tip diameter of 75  $\mu\text{m}$ , and wall thickness of 10  $\mu\text{m}$  arranged in a 4  $\times$  4 (i.e., 16-needle) array with 600- $\mu\text{m}$  needle-to-needle spacing. As shown in the image, the height of each microneedle is similar to the width of a conventional hypodermic needle. Needle arrays of this geometry were used for the insulin delivery experiments described below.

### C. Needle Insertion Mechanics

Successful drug delivery using microneedles requires needles to penetrate living skin and withstand the force of insertion without breaking. An experiment carried out in human subjects using single needles with a geometry equal to those shown in Fig. 5 determined that the average force required to insert the microneedle into skin was approximately 0.2 N (i.e., 20 g). The subjects reported these insertions as painless, although they did cause minor sensation. A separate experiment determined the force required to fracture a microneedle by pressing it against a firm surface; this value was 3 N. Examining the ratio of fracture force to insertion force yields a margin of safety of 15. Although the insertion and fracture forces for an array of needles were not measured, preliminary data suggest that these forces scale directly with the number of needles, as long as the spacing between needles is wide enough for skin deformation caused by one needle not to overlap with that of neighboring needles (data not shown). Altogether, these data indicate that this microneedle design has robust mechanical properties for reliable insertion into skin without breaking.

### D. Insulin Delivery

To test the ability of microneedles to administer drugs, the arrays of hollow microneedles (Fig. 5) were used to deliver insulin to diabetic rats. Changes in blood glucose level and plasma insulin concentration were monitored during and after delivery of insulin through the microneedle arrays.

Fig. 6(a) shows the effect of microneedles on transdermal insulin delivery. After application of the microneedle “patch” and an approximately 30-min lag time, blood glucose level was steadily reduced over 4 h of insulin delivery to 47% of its original value [analysis of variance (ANOVA),  $p < 0.001$ ]. When insulin was subsequently removed from the skin, blood glucose level remained approximately constant during 4 h of postdelivery monitoring (ANOVA,  $p > 0.99$ ). Animals receiving topical insulin without microneedles as a negative control did not show statistically significant changes in blood glucose level (ANOVA,  $p > 0.99$ ). This pharmacodynamic response was similar to that seen following subcutaneous hypodermic injection of 50 mU of insulin and less than that seen for injection of 500 mU of insulin, which were used as positive controls (data not shown) [19].

As a direct measure of insulin delivery, Fig. 6(b) shows plasma insulin concentration as a function of time. The radioimmunoassay used to determine insulin concentration was specific to the human insulin delivered, so that endogenous rat insulin was not detected. Consistent with the blood glucose measurements, insulin was detected in plasma at the 30-min time point and at a higher concentration at the end of the 4-h delivery period. Four hours after insulin was removed from the skin, plasma insulin levels did not change, which suggests slow release from a drug depot within the skin. Negative control experiments showed that topical insulin without microneedles produced undetectable levels of plasma insulin (data not shown).

### E. Interpretation of Insulin Delivery Results

We refer to the microneedle device as a “patch” because its operation is similar to a transdermal patch. Microneedles were

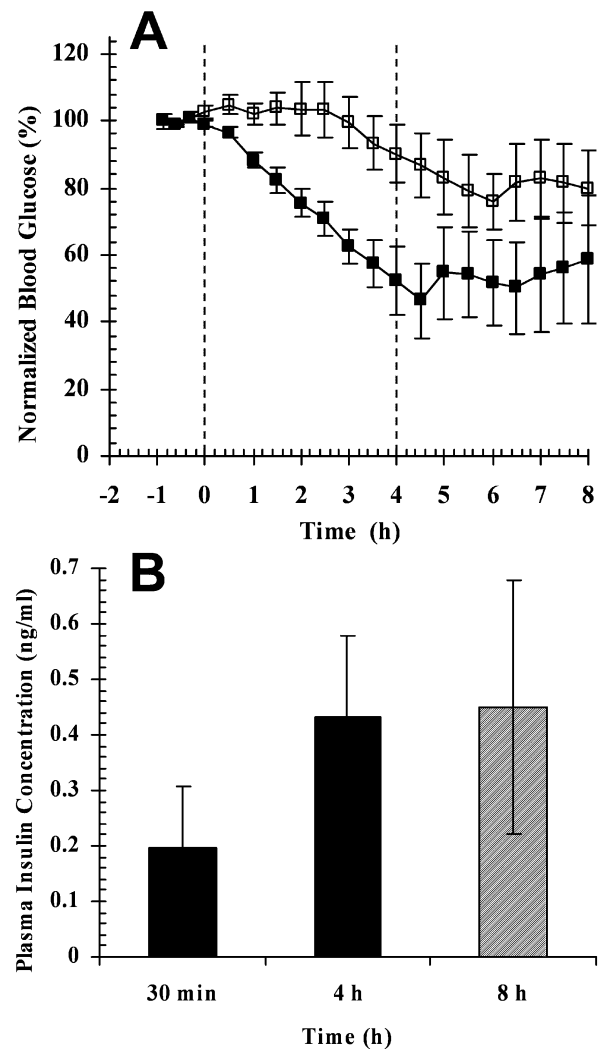


Fig. 6. Effects of transdermal insulin delivery using microneedles on blood glucose level and plasma insulin concentration in diabetic, hairless rats. (a) Blood glucose level before, during, and after transdermal insulin delivery either using microneedles inserted into the skin (■) ( $n = 5$ ) or across intact skin (□) ( $n = 4$ ). Glucose levels are normalized relative to the average blood glucose level during the 1.5-h period before treatment, 465 mg/dl. The dashed lines indicate the beginning and end of the 4-h insulin delivery period. (b) Concentration of human insulin in rat plasma during (0.5 and 4 h, black bars) and after (8 h, gray bar) transdermal delivery using microneedles. Average  $\pm$  SEM is shown for  $n \geq 3$  replicates.

used to pierce across the skin’s outer barrier layer, stratum corneum, and provide conduits through the needle lumens for insulin transport into the skin for capillary absorption and systemic distribution. Insulin delivery was by diffusion over time from a reservoir on the skin surface. Although not done in this study, microneedles can also be used in a manner more like an injection, where a drug solution is actively flowed through the needles and into the skin [17].

The results in Fig. 6(a) should be interpreted with two caveats in mind. First, urethane, which was used to anesthetize the rats, is known to influence blood glucose levels in rodents, where the ability of injected insulin to lower blood glucose levels can be muted by as much as 50% [24], [25]. This suggests that urethane may have reduced the degree to which insulin lowered blood glucose levels in this study. Repeating the same experiment with a different anesthetic might yield more dramatic reductions in blood glucose levels than shown in Fig. 6.

The second caveat concerns comparing measurements of blood glucose levels and measurements of insulin levels in the blood. Blood glucose pharmacodynamic measurements [Fig. 6(a)] suggest that on the order of 50 mU of insulin was delivered by microneedles. In contrast, direct pharmacokinetic measurements [Fig. 6(b)] showed plasma insulin levels of 0.43 ng/ml ( $12 \mu\text{U}/\text{ml}$ ), which corresponds to a dose of 1.4 mU, based on a 0.4 L/kg volume of distribution [26], [27]. This order-of-magnitude difference between pharmacokinetic and pharmacodynamic estimates of the amount of insulin delivered could be explained by a stronger pharmacodynamic response to insulin delivered from microneedles near the capillary loops at the dermal-epidermal junction compared to insulin injected with a hypodermic needle into the subcutaneous space.

#### IV. CONCLUSIONS

To provide arrays of hollow metal microneedles that could be mass produced for minimally invasive drug delivery, we developed a fabrication method to laser-drill a polymer mold, coat the mold with a conductive seed layer, electroplate the mold with metal, and release the metal microneedles by selectively etching the mold. Using this approach, combined with a laser-trepanning technique to produce tapered holes, microneedles were fabricated with a wide range of different geometries. The needle geometry selected for detailed study was shown to insert into skin of human subjects without breaking. Drug delivery experiments using an 16-microneedle array inserted into the skin of diabetic, hairless rats showed that insulin was delivered into the bloodstream and that the blood glucose level was reduced by 47% over a 4-h insulin delivery period. Overall, these results suggest that microneedles can be fabricated for minimally invasive delivery of insulin, or other compounds, for continuous or possibly modulated administration over time.

#### ACKNOWLEDGMENT

The authors would like to thank C. Corley for help with animal studies, as well as D. Ackley for conversations regarding fabrication techniques for large scale manufacturing.

#### REFERENCES

- [1] M. B. Davidson, *Diabetes Mellitus: Diagnosis and Treatment*, 4th ed. Philadelphia, PA: Saunders, 1998.
- [2] A. Liebl, "Challenges in optimal metabolic control of diabetes," *Diabetes Metab. Res. Rev.*, vol. 18, no. 3, pp. S36-S41, 2002.
- [3] M. R. Prausnitz, "Overcoming skin's barrier: The search for effective and user-friendly drug delivery," *Diabetes Technol. Ther.*, vol. 3, pp. 233-236, 2001.
- [4] D. R. Owens, "New horizons—Alternative routes for insulin therapy," *Nat. Rev. Drug Discov.*, vol. 1, pp. 529-540, 2002.
- [5] S. Henry, D. V. McAllister, M. G. Allen, and M. R. Prausnitz, "Microfabricated microneedles: A novel approach to transdermal drug delivery," *J. Pharm. Sci.*, vol. 87, no. 8, pp. 922-925, 1998.
- [6] M. L. Reed, W. Clarence, K. James, S. Watkins, D. A. Vorp, A. Nadeem, L. E. Weiss, K. Rebello, M. Mescher, A. J. C. Smith, W. Rosenblum, and M. D. Feldman, "Micromechanical devices for intravascular drug delivery," *J. Pharm. Sci.*, vol. 87, no. 11, pp. 1387-1393, 1998.
- [7] D. V. McAllister, M. G. Allen, and M. R. Prausnitz, "Microfabricated microneedles for gene and drug delivery," *Annu. Rev. Biomed. Eng.*, vol. 2, pp. 289-313, 2000.
- [8] S. Hashmi, P. Ling, G. Hashmi, M. L. Reed, R. Gaugler, and W. Trimmer, "Genetic transformation of nematodes using arrays of micromechanical piercing structures," *BioTechniques*, vol. 19, no. 5, pp. 766-770, 1995.
- [9] W. Lin, M. Cormier, A. Samiee, A. Griffin, B. Johnson, C. L. Teng, G. E. Hardee, and P. E. Daddona, "Transdermal delivery of antisense oligonucleotides with microprojection patch (Macroflux®) technology," *Pharm. Res.*, vol. 18, no. 12, pp. 1789-1793, 2001.
- [10] J. A. Mikszta, J. B. Alarcon, J. M. Brittingham, D. E. Sutter, R. J. Pettis, and N. G. Harvey, "Improved genetic immunization via micromechanical disruption of skin-barrier function and targeted epidermal delivery," *Nat. Med.*, vol. 8, pp. 415-419, 2002.
- [11] M. R. Prausnitz, "Microneedles for transdermal drug delivery," *Adv. Drug Deliv. Rev.*, vol. 56, pp. 581-587, 2004.
- [12] F. Chabri, K. Bouris, T. Jones, D. Barrow, A. Hann, C. Allender, K. Brain, and J. Birchall, "Microfabricated silicon microneedles for non-viral cutaneous gene delivery," *Br. J. Dermatol.*, vol. 150, pp. 869-877, 2004.
- [13] S. Kaushik, A. H. Hord, D. D. Denson, D. V. McAllister, S. Smitra, M. G. Allen, and M. R. Prausnitz, "Lack of pain associated with microfabricated microneedles," *Anesth. Analg.*, vol. 92, pp. 502-504, 2001.
- [14] L. Lin and A. P. Pisano, "Silicon-processed microneedles," *J. MEMS*, vol. 8, no. 1, pp. 78-84, 1999.
- [15] J. Chen, K. D. Wise, J. F. Hetke, and S. C. Bledsoe Jr, "A multichannel neural probe for selective chemical delivery at the cellular level," *IEEE Trans. Biomed. Eng.*, vol. 44, no. 8, pp. 760-769, Aug. 2001.
- [16] J. G. E. Gardeniers, R. Lutge, J. W. Berenschot, M. J. de Boer, Y. Yeshurun, M. Hefetz, R. van't Oever, and A. van den Berg, "Silicone micromachined hollow microneedles for transdermal liquid transport," *J. MEMS*, vol. 6, no. 1, pp. 855-862, 2003.
- [17] D. V. McAllister, P. M. Wang, S. P. Davis, J.-H. Park, P. J. Canatella, M. G. Allen, and M. R. Prausnitz, "Microfabricated needles for transdermal delivery of macromolecules and nanoparticles: Fabrication methods and transport studies," *Proc. Nat. Acad. Sci.*, vol. 100, pp. 13 755-13 760, 2003.
- [18] S. P. Davis, B. J. Landis, Z. H. Adams, M. G. Allen, and M. R. Prausnitz, "Insertion of microneedles into skin: Measurement and prediction of insertion force and needle fracture force," *J. Biomech.*, vol. 37, pp. 1155-1163, 2004.
- [19] W. Martanto, S. P. Davis, N. R. Holiday, J. Wang, H. S. Gill, and M. R. Prausnitz, "Transdermal delivery of insulin using microneedles *in vivo*," *Pharm. Res.*, vol. 21, no. 6, pp. 947-952, 2004.
- [20] M. Schlesinger and M. Paunovic, *Modern Electroplating*. New York: Wiley, 2000.
- [21] K. C. Tomlinson, S. M. Gardiner, R. A. Hebden, and T. Bennett, "Functional consequences of streptozotocin-induced diabetes mellitus, with particular reference to the cardiovascular system," *Pharmacol. Rev.*, vol. 44, pp. 103-150, 1992.
- [22] P. J. Rousche and R. A. Normann, "A method for pneumatically inserting an array of penetrating electrodes into cortical tissue," *Ann. Biomed. Eng.*, vol. 20, pp. 413-22, 1992.
- [23] H. I. Maibach and T. Menne, *Nickel and the Skin: Immunology and Toxicology*. Boca Raton, FL: CRC, 1989.
- [24] A. Sanchez-Pozo, J. C. Alados, and F. Sanchez-Medina, "Metabolic changes induced by urethane-anesthesia in rats," *Gen. Pharmacol.*, vol. 19, pp. 281-284, 1988.
- [25] M. Y. Wang, L. M. Ren, Z. J. Du, and S. X. Fu, "Urethane-induced hyperglycemia," *Acta Pharmacol. Sin.*, vol. 21, pp. 271-275, 2000.
- [26] K. Bachmann, D. Pardoe, and D. White, "Scaling basic toxicokinetic parameters from rat to man," *Environ. Health Perspect.*, vol. 104, pp. 400-407, 1996.
- [27] D. W. Sifton, *Physicians' Desk Reference*, 52nd ed. Montvale, NJ: Thomson PDR, 2003.

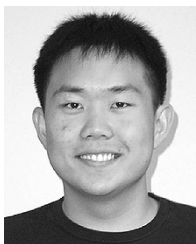


**Shawn P. Davis** was born in Spokane, WA, in 1976. He received the B.Sc. degree in chemical engineering from the Florida Institute of Technology, Melbourne, in 1998. He received the Ph.D. degree in chemical engineering from the Georgia Institute of Technology, Atlanta, in 2004.

His work experience includes an internship with the Washington Internships for Students of Engineering during the summer of 1997 in Washington, DC. He then worked as a Research Engineer for Redeon, Inc., of Burlington, MA, during 2000-2001.

He is currently a Development Engineer for Milliken & Company of Spartanburg, SC.

Dr. Davis is a member of the American Institute of Chemical Engineers and the American Society of Mechanical Engineers.



**Wijaya Martanto** was born in Semarang, Indonesia, in 1979. He received the B.S. degree (*magna cum laude* with high distinction) in chemical engineering from the University of Minnesota, Minneapolis, in 2000. He is currently working towards the Ph.D. degree in the School of Chemical & Biomolecular Engineering, Georgia Institute of Technology, Atlanta.

His current research interests include fluid flow through microneedles, and transdermal drug delivery using microneedles.



**Mark G. Allen** (M'89–SM'04) received the Ph.D. degree in microelectronics from the Massachusetts Institute of Technology, Cambridge, in 1989; the S.M. degree in chemical engineering from the Massachusetts Institute of Technology in 1986; and B.S.E. and B.A. degrees in electrical engineering, chemical engineering, and chemistry from the University of Pennsylvania, Philadelphia, in 1984 and 1988, respectively.

He holds the J.M. Pettit Professorship in Microelectronics in the School of Electrical and Computer Engineering at the Georgia Institute of Technology, Atlanta and a joint appointment in the School of Chemical and Biomolecular Engineering. He has also held visiting professorships at the Swiss Federal Institute of Technology, Zurich, Switzerland (ETH-Zurich). His research interests are in the area of microfabrication and nanofabrication technology, with emphasis on new approaches to fabricate structures, sensors, and actuators with characteristic lengths in the micro- to nanoscale from both silicon and nonsilicon materials. Examples include micromagnetics, bioimplantable microdevices, high-temperature sensors, small-scale power generation, compact actuators, fluidic microvasculatures, and the use of microstructures to create nanostructures.

Prof. Allen was General Co-Chair of the 1996 IEEE Microelectromechanical Systems Conference.



**Mark R. Prausnitz** received the B.S. degree from Stanford University, Stanford, CA, in 1988 and the Ph.D. degree from the Massachusetts Institute of Technology, Cambridge, in 1994, both in the field of chemical engineering.

He is currently an Associate Professor of Chemical and Biomedical Engineering at the Georgia Institute of Technology, Atlanta. He previously worked as a Biomedical Engineer for ORBIS International, a Junior Chemical Engineer at ALZA Corporation, and an Instructor of technical communication at Stanford

University. His research interests address the application of engineering tools to solve drug delivery problems, especially in the context of microfabricated devices for transdermal drug delivery and ultrasound-based mechanisms for intracellular delivery of drugs and genes.

Prof. Prausnitz has received a number of awards, including the Curtis W. McGraw Research Award from the American Society for Engineering Education (2004), the CAREER Young Investigator Award from the National Science Foundation (1996), and the Outstanding Pharmaceutical Paper Award from the Controlled Release Society (1992). In 2002, he served as the NSF/NIH Scholar-in-Residence at the National Institutes of Health.